CHANGES IN DNA CONFORMATION AND TYPES OF MUTATION INDUCED IN CHO *dhfr* GENE BY N-2-ACETYLAMINOFLUORENE AND N-2-AMINOFLUORENE

Dezider Grunberger and Adelaide M. Carothers

Institute of Cancer Research, College of Physicians and Surgeons,
Columbia University, 701 West 168th Street, New York, NY 10032

Dedicated to the memory of Professor František Šorm.

Neoplastic development in vivo is a multistage process consisting generally of at least three operationally defined stages; initiation, promotion, and progression[1,2]. The prevailing view is that the initiation process in most systems involves a mutational event. The mutational basis of initiation is supported by studies in several systems such as the mouse skin or mammary carcinomas[3-5]. In both of these systems a carcinogen-induced mutation of the *ras* proto-oncogene resulted in an active oncogene[4,5].

The initiation phase of chemical carcinogenesis often involves metabolic activation of the chemical initiator to yield an electrophile that forms covalent adducts with nucleophilic residues in DNA (ref.[6]). A consequence of the binding of the carcinogen to DNA is a change in its primary structure, as well as in its conformation at the sites of modification which, in turn, can lead to mutation[7,8].

To study the correlation between the changes in DNA structure and types of mutation induced by chemical carcinogens we have chosen a very potent hepatocarcinogen, N-2-acetylaminofluorene (AAF). This carcinogen is metabolically activated in most tissues by the cytochrome P-450 system to N-hydroxy-AAF which is further metabolized to the ultimate carcinogenic form to a sulfate or acetoxy-ester[8-10]. These highly reactive esters bind covalently to DNA predominately at the C-8 position of guanosine residues[11] in acetylated (AAF) or deacetylated-N-2-aminofluorene form (AF). There is also a minor adduct at N^2 position of G (ref.[12]).

Conformation of DNA Modified by AAF

Molecular model building of AAF modified oligonucleotides, circular dichroism and nuclear magnetic resonance (NMR) spectra in combination with enzymatic studies provided considerable evidence that AAF modification of the C-8 position of G results in a dramatic conformational distortion at the modification site[13-16].

On the basis of these results, we proposed a specific, three-dimensional conforma-tion called the "base displacement" model[17]. The first feature of this model is that the attachment of the AAF residue to the C-8 position of G is associated with a change in the glycosidic N9—C1′ conformation from the *anti* form of nucleosides in nucleic acids with Watson–Crick geometry to the *syn* form (Fig. 2). The second major feature of this model is that there is a stacking interaction between AAF and the base adjacent to the substituted G residue. These changes are best illustrated in a computer-generated stereoscopic display of a double stranded DNA fragment (Fig. 1). In the display, the modified base has been rotated around the glycosidic
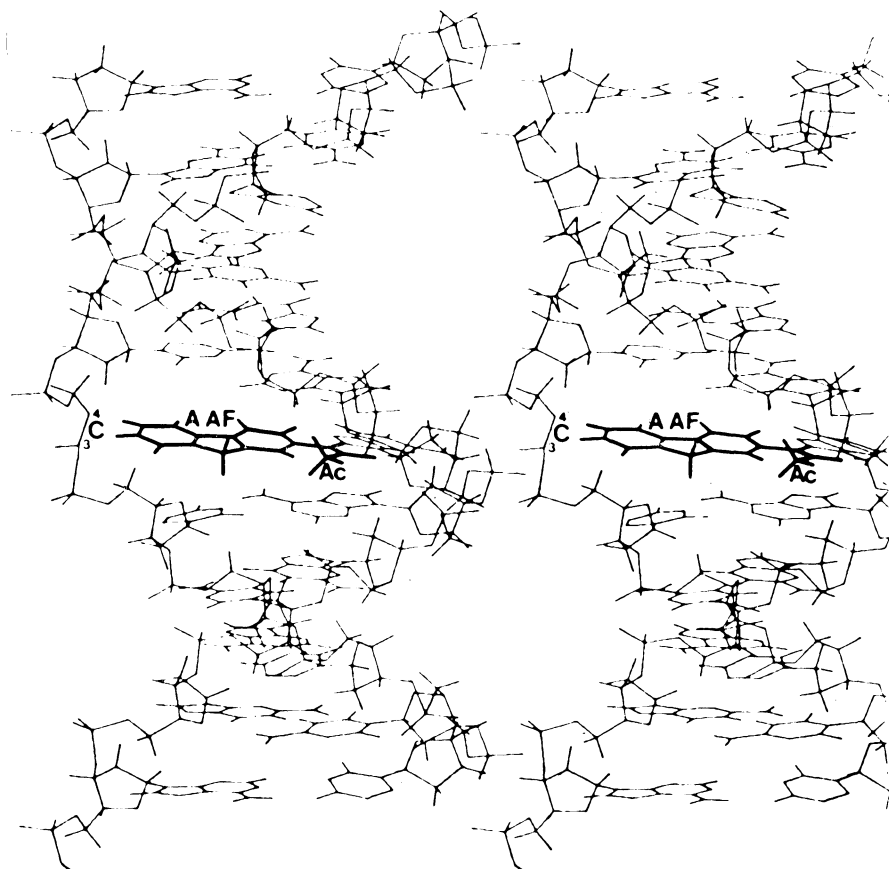

FIG. 1

Computer generated stereoscopic display of the base-displacement model of DNA modified by AAF

bond from *anti* to *syn* conformation to avoid any steric hindrance. In addition, the planar fluorene ring system is inserted into the helix occupying the position formerly held by the displaced guanine residue. It is also evident that the G residue displaced by AAF in the double helix cannot base pair with the C residue on the complementary strand and that during the process of replication or transcription no base pairing at this position can occur. A similar model, called the "insertion–denaturation model" has been proposed by Fuchs and Daune[18].

Since attachment of AAF to G residues requires rotation of the base about the glycosidic bond and there is less hindrance to the rotation of bases in single stranded than in double stranded regions, it follows that single-stranded regions of nucleic acids are more susceptible to AAF modification than double-stranded ones[16,19]. The base displacement model was confirmed by Broyde and Hingerty[20] using
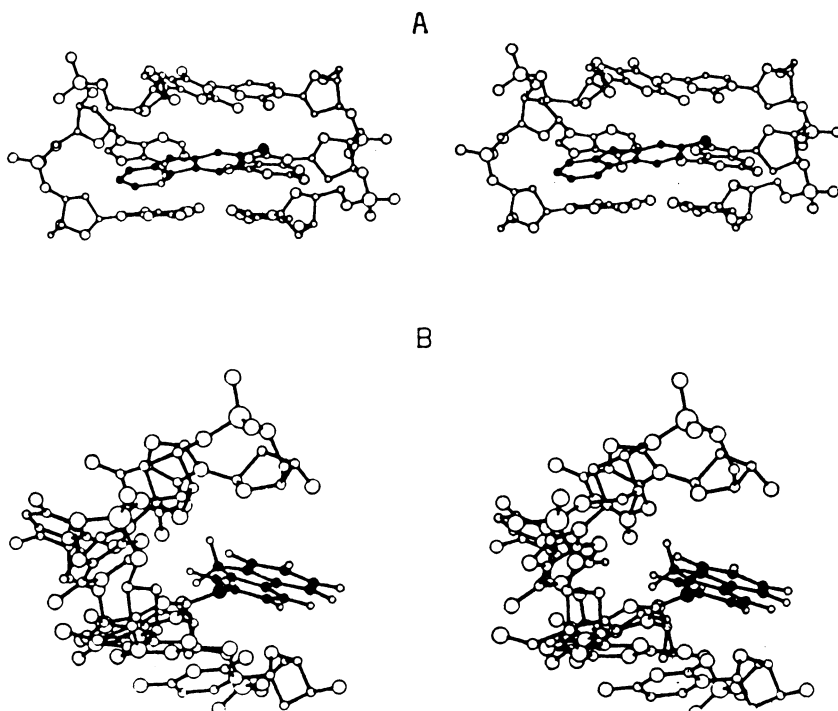
A

B

FIG. 2

Two stereoviews of the [C-G(AF)-C] : [G-A-G] trinucleotide segment of the 11-mer at neutral pH. View A emphasizes the location of AF in the minor groove and the extension of the AF ring toward the sugar-phosphate backbone on the partner strand. View B emphasizes the interaction of AF with the walls of the minor groove. [From ref.[25]]

minimized potential energy calculations for dCpdG modified with AAF. For all computed conformers with energies less than 21 kJ/mole, the fluorene ring is stacked approximately coplanar with the neighboring cytidine, the G residue is *syn* and the plane of G is twisted perpendicular to the plane of the fluorene. These data are in agreement with our experimental findings that led to the base displacement model.

Conformation of DNA Modified by AF

After in vivo adminstration of N-OH-AAF, a major fraction of the DNA-bound carcinogen in rat liver is deacetylated[21-23]. This lesion has been identified as N-(deoxyguanosin-8-yl)-2-AF and it is accumulated in the target tissues (Fig. 1). Differences in biological properties between C8-G-AAF and C8-G-AF adducts in DNA [for example, the different rates of excision repair of AAF- and AF-G (ref.[24])] may be related to different conformational alterations in DNA. The deacetylated adduct may cause less distortion in the duplex molecule than the acetylated one.

For the study of the conformation of AF-modified DNA, we have applied 2-dimensional NMR of a complementary duplex[25]. Since it has been shown that very often in the process of replication an A is inserted opposite a noninstructional base, as G(AF) (ref.[37]), and also that AF induced predominantly a G → T transversion mutation[26,27], our approach focused on NMR studies of a DNA oligomer containing an adenosine in the center of the duplex opposite a G(AF) lesion. The oligomer used was an 11-mer duplex d[C-C-A-T-C-G(AF)-C-T-A-C-C]: d[G-G-T-A-G-A-G-A--T-G-G] (ref.[25]). The experimental NMR distance constraints were combined with energy minimization calculations to define the conformations centered about the G(AF) : A lesion site in the 11-mer duplex.

The stereoview (Fig. 2) of the [C-G(AF)-C] : [G-A-G] trinucleotide segment in the center of the 11-mer demonstrates the location of AF in the minor groove and the extension of the AF ring toward the sugar-phosphate backbone on the partner strand. Positioning of the AF in the minor groove can only occur if G(AF) adopts a *syn* glycosidic torsion angle. The observed nuclear Overhausen effect (NOE) data were in agreement with this conclusion. By switching to a *syn* conformation at G(AF) [*syn*] the bulky AF ligand can be positioned in the minor groove resulting in the formation of an G(AF)[*syn*] : A [*anti*] pair without major disruption of the helix. This alignment is illustrated in a ball and stick stereo drawing in Fig. 3 (top) and a space filling stereo drawing in Fig. 3 (bottom). In this conformation an interplay between hydrophobic interactions and hydrogen-bonding contributes to the stabilization at the modification site. The neutral pH conformation is stabilized only by hydrophobic interactions between the AF ring and the walls of the minor groove without hydrogen bonds between G(AF)) and A in the partner strand (Fig. 3A). At acidic pH, a single hydrogen bond was proposed linking the N1 of protonated A and O6 of G(AF) (Fig. 3B). A major difference in these alignments is that the
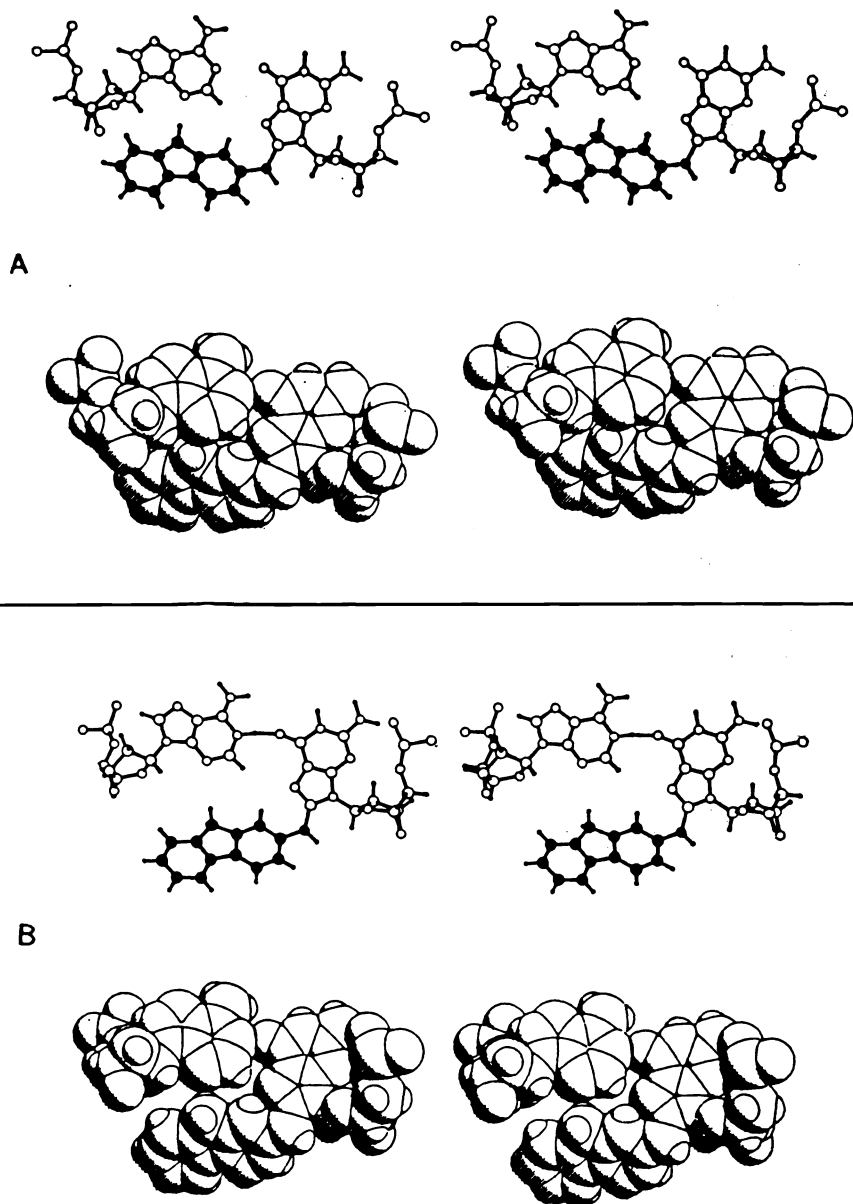
FIG. 3

A ball and stick (top) and space-filling (bottom) stereoview of the pairing alignment at the G(AF)[syn] : A[anti] lesion site in the 11-mer at neutral pH (A) and at acidic pH (B). [From ref.[25]]

aromatic ring of aminofluorene pivots away from the helix axis at the acidic pH and breaks the contacts observed with the G16-A17-G18 segment on the partner strand in the neutral pH conformation. The neutral pH conformation of the AF-modified 11-mer is illustrated on the computer generated stereoview drawing in Fig. 4. It is evident from this figure that only the region of G(AF) : A pair has been changed as shown in Fig. 2; the rest of the molecule remained in an overall B-DNA type structure.

Interestingly, in bacterial systems it has been shown that G(AF) adduct induces predominantly a G : C → T : A transversion. A mechanism that could dictate this high degree of mutational specificity is the incorporation of an A base opposite the AF-modified G in DNA during replication. Thus, the results of our conformational studies support the idea that conformational aspects of carcinogen-modified bases have an impact on the mutational spectra.

Mutations Induced by N-Acetoxy-AAF at the CHO DHFR Locus

To study the possible correlation between the conformation of AAF and AF modified DNA and types of mutations, we have used the dihydrofolate reductase (*dhfr*) gene in Chinese hamster ovary (CHO) cells[27]. The dhfr gene displays typical mammalian gene organization, being comprised of six exons spanning 25 kb (ref.[28]). The *dhfr* gene product is an enzyme that maintains the cellular level of tetrahydrofolic
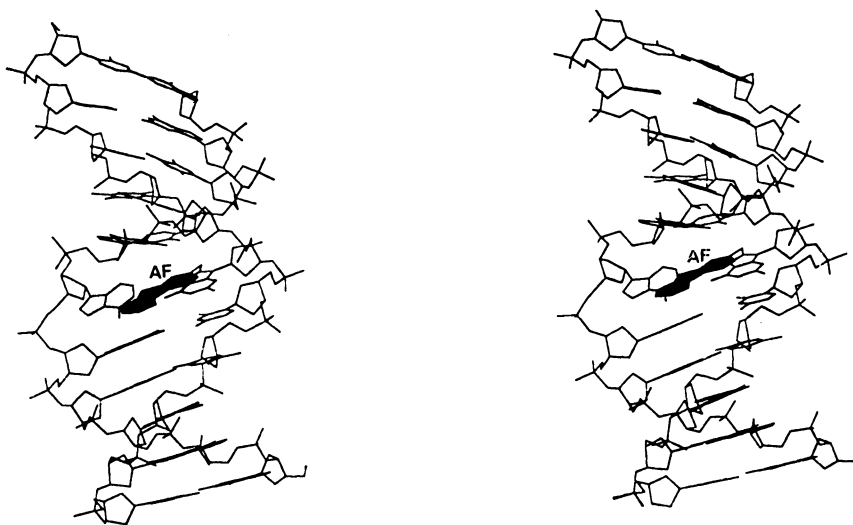

FIG. 4

Stereoview of the AF-modified 11-mer. The AF ring is black (Courtesy of Dr S. Broyde)

acid, a cofactor that functions in one-carbon transfer reactions. The selection scheme for enzyme-deficient mutants is based on the role of DHFR in the de novo synthesis of glycine, purine nucleotides, and thymidylate. The selective agent is labeled with a high specific activity [^{3}H]deoxyuridine (24 Ci/mmol). The metabolic conversion of [^{3}H]dUrd to [^{3}H]dTMP leads to incorporation of labeled TMP into DNA where its subsequent radioactive decay is lethal to DHFR$^+$ cells. Mutants which are *dhfr$^-$* cannot mediate this conversion and therefore survive. Individual colonies that survives the selection are isolated and the cells tested for glycine, thymidine, and hypoxanthine auxotrophy. Only one mutant per dish displaying such auxotrophy is analyzed further. Each of the putatively DHFR$^-$ clones is then assayed for failure to bind a substrate analog, [^{3}H]-methotrexate.

Southern Blot Analysis of DHFR Mutant DNA

From three separate treatments of cells with N-acetoxy-AAF, a total of 29 independent mutants were isolated. The conditions for mutagenesis yielded about 35% survival of the treated cells. The induced frequency of mutation was $1.5 \cdot 10^{-5}$; the spontaneous rate is $1.3 \cdot 10^{-7}$ (refs[29,30]). The 25 kb CHO *dhfr* gene has been previously cloned and mapped[28]. DNA from the mutants were analyzed by Southern blotting[31]. An example of the initial screening of several N-acetoxy-AAF-induced mutants is depicted in Fig. 5. The mutant genomic DNA were cut with the restriction
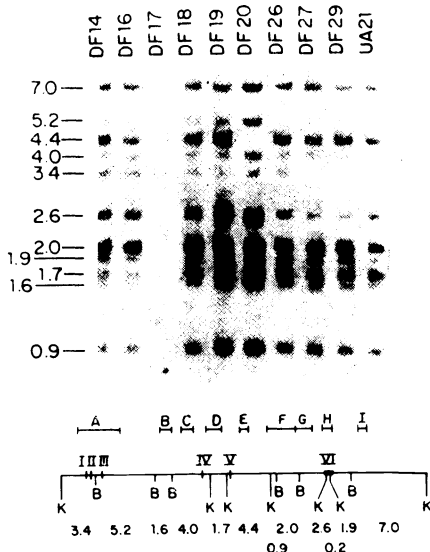

FIG. 5

Southern blot analysis of *dhfr* gene in DNA samples from AAF induced *dhfr$^-$* mutants (Upper). DNAs were digested by KpnI and BstEII. A map of the 34-kb sequence scanned by the mixed probe, showing the location of KpnI (K) and BstEII (B) cleavage sites (Lower). The mixed probe is represented by lines A—I drawn above the *dhfr* fragments to which they hybridize. [From ref.[30]]

endonucleases **KpnI** and **BstEII**. These enzymes create 12 bands that span a conti-nuous 34 kb containing the *dhfr* locus. Southern blots of these bands resolved on agarose gels were hybridized to a mixed probe consisting of 10 fragments derived from *dhfr* recombinant plasmids[30]. Components of the mixed probe are represented by lines lettered A-I drawn above the fragments to which they hybridize. If the DNA banding pattern of a mutant was identical to that of the parental cell line, UA21, it was designated as carrying a small lesion possible a frameshift or point mutation. Sequence changes of 100 bp or less are below the resolution limit of this technique. N-acetoxy-AAF mutagenesis induced structurally different types of lesions in the *dhfr* gene. Three mutants with gross alterations in the gene are shown in Fig. 5. A complete deletion (>34 kb) has occurred in DF17. Another mutant, DF20, has lost the 4·4 kb **KpnI** fragment and a new band of 2·3 kb is evident. The 3·4 kb fragment containing the 5′ end of the gene is missing in DF27.

Results of Southern blot analysis of 29 mutants using the mixed probe are sum-marized in Table I. Point mutations or small (<100 bp) deletions or insertions were found to have occurred in 72% of the mutant clones; the remainder (28%) carried large deletions and rearrangements. The HPLC analysis of modified nucleosides obtained from DNA UA21 cells roughly 2 hours after N-acetoxy-AAF treatment indicated that the ratio of dG-AAF to dG-AF (12 : 88) is similar to the ratio of gross- to small-lesion *dhfr* mutants. Although it is not feasible to ascertain the ratio of adducts during the period in which the treated cells recover and replicate, there may be a correlation between the conformational alterations induced in DNA by dG-AAF and dG-AF and the types of mutations we have identified at the *dhfr* locus.

Mapping and DNA *Sequencing of* N-*Acetoxy-*AAF-*Induced Point Mutations*

To determine the exact DNA base change in each point mutant, a DNA fragment containing the mutated sequence was purified by amplifying the relevant region by the polymerase chain reaction (PCR) method[32]. Since most of the base changes in the gene are restricted to the protein coding sequence, it appeared more efficient to sequence *dhfr* mRNA than genomic fragments that span each individual exon[33]. Drawn in Fig. 6 is a representation of the approach. The cDNA amplification primers ("amplimers") are 20 base oligonucleotides; both the 3′ and 5′ amplimers are homologous to untranslated sequences of the *dhfr* mRNA. The sequence homo-logous to the 5′ amplimer originates 57 bases upstream of the AUG, and that which is homologous to the 3′ amplimer originates 112 bases downstream of the UAA codon. The 3′ amplimer is first added to total RNA to synthesize cDNA in the presence of reverse transcriptase. Both 5′ and 3′ amplimers are then combined in equal molar amounts for PCR in order to maximize the DNA yield. We designed sequencing primers to divide the 730 bp *dhfr* cDNA into units of approximately 250 bases,

a size that can be reliably read from a single sample loading on a sequencing gel. The sequencing primer 3 hybridizes to the nontranscribed cDNA strand 20 bases downstream of the termination codon. Separate sequencing reactions performed

TABLE I

Structurally different types of mutations induced by AAF in the *dhfr* gene

	Type of mutation	Total
	Small mutations[a]	21
	Deletions	6
	Rearrangements[b]	2

[a] Single base pair changes, small insertions or deletions <100 base pairs; [b] disruptions, i.e. translocation, large insertion, duplication, or inversion.
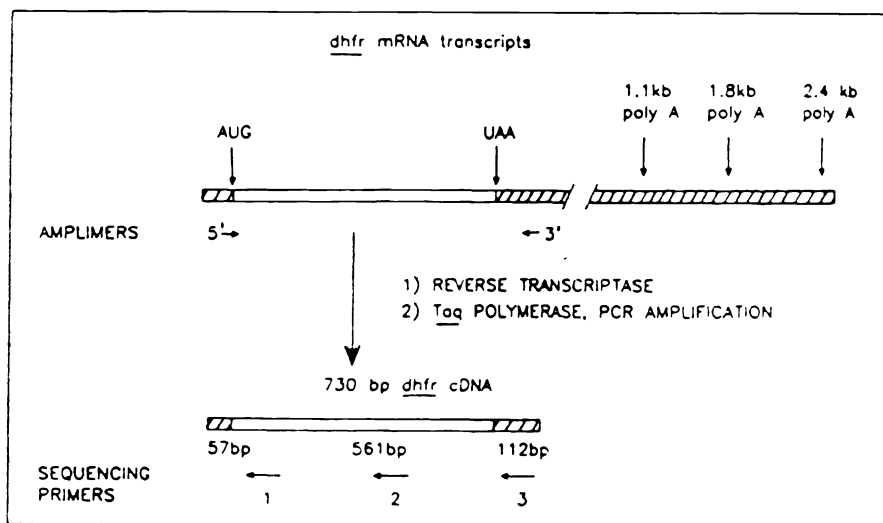

FIG. 6

Strategy for *dhfr* cDNA synthesis and sequencing. The three species of mature *dhfr* mRNA are drawn above. Hatch-marked areas indicate nontranslated regions. The relative locations of the synthetic 20-mer oligonucleotides for priming cDNA synthesis and subsequent PCR are shown below. At the bottom is shown a representation of *dhfr* cDNA. Relative locations of sequences homologous to the coding strand that were synthesized for use as sequencing primers are indicated as numbered arrows. The sequence of primers 1—3 in 5′ to 3′ orientation are: AAAGGTCGA. .TTCTTCTCAGG, AGAGTCTGAGATGGCCTGGC and AAGCAGTAGAACTTGAAGTC, respectively. [From ref.[33]]

with mutant cDNA and primers 1—3, yield the entire *dhfr* coding sequence and use 12 lanes of a gel.

A demonstration of the procedure for mutant analysis starting from genomic DNA is shown in Fig. 7 and illustrates the relative locations and sizes of the segments chosen for amplification (bottom). As an example, the result of PCR amplification of exon VI sequences from different mutants appears in the upper left portion of the figure. On the right side, is presented the data of direct DNA sequencing of the corresponding mutants (except DF40). In this experiment, the sites of 3 mutations were identified (DF18, DF8, DF31) and are indicated by arrows, whereas a wild-type sequence was evident for this region of the gene in 2 other mutants (DF11, DF47).
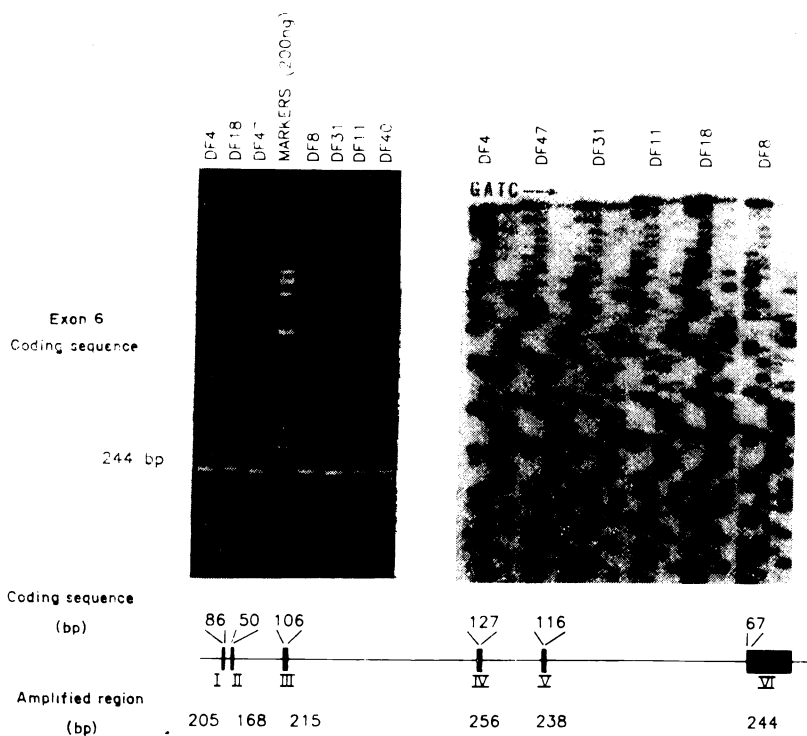

FIG. 7

Direct sequencing of PCR-amplified mutant DNA. Top left: amplification of a region sequencing the coding region of exon VI of *dhfr* gene in 7 mutants. Top right: sequencing gel of the amplified fragments. Bottom: map of the *dhfr* gene showing, above the map, the size of each exon and below the map, the sizes of the exon-spanning fragments that were amplified. [From ref.[34]]

A summary of the results of DNA sequencing of the complete set of N-acetoxy-
-AAF-induced putative point mutants is shown in Table II (ref.[34]). In all cases, base
changes involving guanine bases occurred within the *dhfr* coding sequence or at
splice site consensus sequences. Of the base substitution mutations, 83% (15/18)
were G : C → T : A and 6% (1/18) G : C → C : G transversions; the remaining 11%

TABLE II
Characteristics of AAAF-induced mutants

Designation	Target sequence	Change	Exon	Position	Phenotype	mRNA level
A. *Base substitutions*						
DF47	ACGGCGA*	G → T	1	29	Missense: Ala_9-Asp	Normal
DF3	GTGGAAG	G → T	2	133	Nonsense: ochre	<10%
DF12X1	CTGGAAG	G → T	2	133	Nonsense: ochre	<10%
DF5	CTGGAAG	G → T	2	133	Nonsense: ochre	<10%
DF30	CCTGGTT	G → C	3	173	Missense: Trp_{57}-Ser	Normal
DF26	AGAGAGC	G → T	3	235	Nonsense: amber	<10%
DF40	TAAGTGA	G → A	3	+5	Splice donor defect	<10%
DF19	TCAGGGA	G → T	4	−1	Splice accept defect	<10%
DF43	AGGGAAC	G → T	4	244	Nonsense: ochre	<10%
DF11	TTGGAGG	G → T	4	350	Missense Gly_{116}-Val	Normal
DF29	TTGGAGG	G → T	4	350	Missense: Gly_{116}-Val	Normal
DF35	CTTGTCA*	G → T	5	410	Missense: Thr_{136}-Lys	Normal
DF44	AGAGTAA	G → T	5	+1	Splice donor defect	Normal
DF32	TCTGAAG	G → T	6	505	Nonsense: ochre	Normal
DF8	CCTGGAC*	G → A	6	511	Nonsense: amber	Normal
DF31	GAGGAAA	G → T	6	517	Nonsense: ochre	Normal
DF42	TTTGAAG	G → T	6	541	Nonsense: ochre	Normal
DF14	TATGAGA	G → T	6	550	Nonsense: amber	Normal
B. *Frameshifts*						
DF16	CAAGAAC	−G	1	57	Nonsense at 113: opal	<10%
DF18	AAGG∧CAT	+A	6	524	Nonsense at 534: ochre	Normal

The sequence surrounding the presumed target G base (semi-bold) is given. An asterisk denotes
the sequence is from the non-coding (template) strand; otherwise, the sequence is from the
coding (non-template) strand. All sequences are written 5' to 3'. The position numbers refer to
the cDNA sequence, where the 1st base is the A of the ATG translation initiation codon. For
mutations that fall in introns, the position relative to the nearest exon is given, + indicating
downstream from the exon and − meaning upstream. The level of mRNA is described as normal
if it was at least 50% of the wild-type value.

(2/18) were G : C → A : T transition. Two frameshift mutations were found in the 20 mutants analyzed. In one case, an A : T base pair was inserted and in the other, a G : C base pair was deleted. The affected G which was presumably carcinogen--modified and changed as a result of mutation was on the coding strand in 85% of the cases listed. Asterisks denote the three exceptions in which the modified G was on the template strand.

RNA *Phenotypes of dhfr Point Mutants*

The location of point mutations, as well as the relative steady-state levels of *dhfr* mRNA in N-acetoxy-AAF-induced mutants is presented in Table II and was deter- mined by RNase heteroduplex mapping prior to DNA sequencing[34,35]. The results are summarized and illustrated in Fig. 8. The mutants can be placed into three categories based on their RNA phenotypes: *1*) mutants with a wild-type level of RNA having no apparent processing defects, *2*) a splicing mutant with wild-type levels of *dhfr* mRNA that skip exons 5 (DF44), and *3*) low-RNA mutants whose steady-state level of *dhfr* transcripts is generally 5−10% that of wild-type cells. The mutants in categories 1 and 2 carry either missense mutations in any of the *dhfr* exons, or nonsense mutations in exon VI, the last exon of the gene. The skipping of exon V (DF44) creates downstream nonsense in exon VI. Their DHFR-deficient phenotype can be ascribed to an impaired function of the DHFR enzyme. The mutants in category 3 have been affected in aspects of gene expression, as well as enzymatic function. About a third of the mutants examined contain a much reduced steady-state level of *dhfr* mRNA. Without exception these mutations have one sequence change in common: all produce a nonsense codon directly or as a result of a frame shift either by + or − base insertion or deletion or by defective splicing.

A decrease in steady-state RNA can arise either at the level of mRNA transcrip- tion, processing, or stability. No difference in transcription rate or in mature mRNA stability was found[36]. The most likely nuclear processing event to be coupled to the cytoplasmic process of translation is nuclear transport. Urlaub et al.[36] have proposed a model in which pre-mRNA begins to exit from the nucleus via a nuclear pore. As its 5′ and emerges from the nucleus, ribosomes immediately begin translating the pre-mRNA, and this protein synthetic operation facilitates the movement of the RNA not only out of the nucleus but through the splicing machinery, as well. When the ribosomes encounters a nonsense codon, this pulling action stops. The delayed egress from the nucleus, leaves the transcript vulnerable to degradation. The involve- ment of splicing in this model is necessary to explain why nonsense codons in exon VI have no effect on *dhfr* mRNA levels. By the time a ribosome reaches exon VI, all splicing has been completed, and the mature mRNA is free to rapidly diffuse out of the nucleus.

Conclusion

We have examined changes in conformation of DNA modified by potent hepatocarcinogens AAF and AF and related these changes to the types of mutations induced
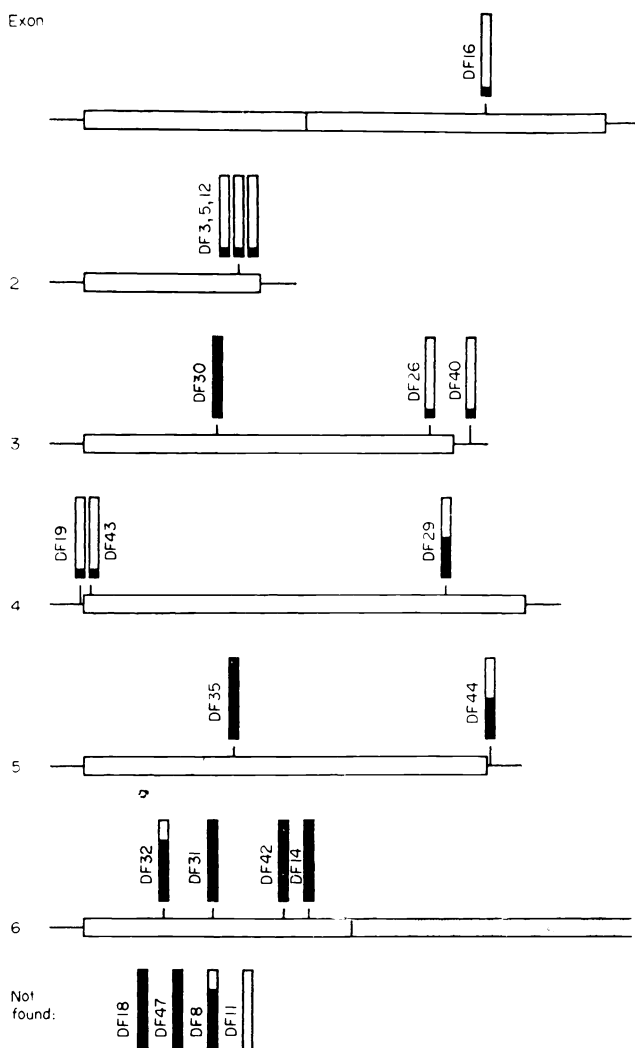

FIG. 8

Map of mutations and the *dhfr* mRNA levels present in each mutant. The bases indicate the 6 exons of the gene and the lines represent intron sequences. The vertical bar above each mutation is used to show the steady-state content of *dhfr* mRNA relative to the parental cells. A complete bar represents 100% of the parental level. [From ref.[34]]

in the *dhfr* gene of CHO cells. Both carcinogens bind preferentially at the C-8 position of dG residue. Modification of DNA by AAF results in a large distortion of the helix which we termed "base displacement." In this conformation, the carcinogen is inserted into DNA perpendicular to the helix axis with the dG in the *syn* form displaced to the outside. As a result of the distorted structure one may expect mainly gross types of mutations (insertion, deletion, translocation or inversion) induced in a gene. In accordance with this assumption, we found in 28% of *dhfr⁻* mutants of CHO cells induced by N-acetoxy-AAF that large deletions and chromosal rearrangements had occurred. This number correlates closely with the 12% dG-AAF adducts detected in DNA of AAF-treated cells. The remaining 88% of the DNA adducts were deacetylated in the form of dG-AF.

The conformation of DNA modified by AF has been established by two-dimensional NMR and energy minimized computations of an 11-mer duplex containing the dG(AF) adduct on one strand positioned across from adenosine in the complementary strand. In the proposed conformation the observed dG(AF)[*syn*] : A[*anti*] alignment results in positioning of the aminofluorene ring in the minor groove. There is an interplay between hydrophobic interactions and hydrogen-bonding contributions to the stabilization at the modification site. The neutral pH conformation is stabilized by hydrophobic interactions between the AF ring and the walls of the minor groove. The acidic pH conformation is stabilized, in part, by a single hydrogen bond between the O6 of G(AF) and N1 of opposite A while retaining the G(AF)[*syn*] : A[*anti*] alignment.

In correlation with the proposed DNA-AF conformation the most frequent type of mutation is a G → T transversion which occurred in 75% of *dhfr⁻* mutants. Similarly, in bacterial systems, others have also determined that dG-AF adduct induces predominantly this type of base substitution[26]. Thus, our results support the idea that conformational aspects of carcinogen-modified bases have an impact on the mutational spectra.

REFERENCES

1. Farber E.: Cancer Res. *44*, 4217 (1984).
2. Weinstein I. B.: Cancer Res. *48*, 4135 (1988).
3. Barrett J. C., Ts'o P. O. P.: Proc. Natl. Acad. Sci. U.S.A. *75*, 3297 (1974).
4. Balmain A., Pragnell I. B.: Nature *303*, 72 (1983).
5. Zarbl H., Sukumar S., Arthur A. V., Martin-Zanca D., Barbacid M.: Nature *315*, 382 (1985).
6. Miller E.: Cancer Res. *38*, 1479 (1978).
7. Miller J. A.: Cancer Res. *30*, 559 (1970).

8. Miller E. C., Miller J. A.: Cancer *47*, 2327 (1981).
9. King C. M., Olive C. W.: Cancer Res. *35*, 906 (1975).
10. Johanson E. F., Levitt D. S., Muller-Eberhard U., Thorgeirsson S. S.: Cancer Res. *40*, 4456 (1980).
11. Kriek E., Miller J. A., Juhl U., Miller E. C.: Biochemistry *6*, 177, (1967).
12. Westra J. G., Kriek E., Hittenhausen H.: Chem.-Biol. Interactions *15*, 149 (1976).
13. Grunberger D., Nelson J. H., Cantor C. R., Weinstein I. B.: Proc. Natl. Acad. Sci. U.S.A· *66*, 488 (1970).
14. Nelson J. H., Grunberger D., Cantor C. R., Weinstein I. B.: J. Mol. Biol. *62*, 331, (1971).
15. Grunberger D., Blobstein S. H., Weinstein I. B.: J. Mol. Biol. *82*, 459, (1974).
16. Levine A. F., Fink L. M., Weinstein I. B., Grunberger D.: Cancer Res. *34*, 319 (1974).
17. Grunberger D., Weinstein I. B. in: *Biology of Radiation Carcinogenesis* (J. M. Yuhas and J. D. Regan, Eds), pp. 175—187. Raven Press, New York 1976.
18. Fuchs R., Daune M.: Biochemistry *11*, 2659 (1972).
19. Fujimura S., Grunberger D., Carvajal G., Weinstein I. B.: Biochemistry *11*, 3629 (1972).
20. Broyde S., Hingerty B. E.: Chem.-Biol. Interactions *40*, 113 (1982).
21. Wirth P. J., Thorgeirsson S. S.: Mol. Pharmacol. *19*, 337 (1980).
22. Beranek D. T., White G. L., Heflich R. H., Beland F. A.: Proc. Natl. Acad. Sci. U.S.A. *79*, 5175 (1982).
23. Schut H. A. J., Wirth P. J., Thorgeirsson S. S.: Mol. Pharmacol. *14*, 682 (1978).
24. Howard P. C., Casciano D. A., Beland F. A., Shaddock J. G. Jr: Carcinogenesis *2*, 97 (1981).
25. Norman D., Abuaf P., Hingerty B. E., Live D., Grunberger D., Broyde S., Patel D. J.: Biochemistry *28*, 7462 (1989).
26. Bichara M., Fuchs R. P. P.: J. Mol. Biol. *183*, 341 (1985).
27. Urlaub G., Kas E., Carothers A., Chasin L.: Cell *33*, 405 (1983).
28. Carothers A., Urlaub G., Ellis N., Chasin L.: Nucleic Acids Res. *11*, 1997 (1983).
29. Mitchell P., Urlaub G., Chasin L.: Mol. Cell. Biol. *6*, 1926 (1986).
30. Carothers A. M., Urlaub G., Steigerwalt R. W., Chasin L. A., Grunberger D.: Proc. Natl. Natl. Acad. Sci. U.S.A. *83*, 6519 (1986).
31. Southern E. M.: J. Mol. Biol. *98*, 503 (1975).
32. Saiki R. K., Gelfand D. N., Stoffel S., Scharf S. J., Higuchi R., Horn G. T., Mullis K. B., Ehrlich H. A.: Science *239*, 487 (1988).
33. Carothers A. M., Urlaub G., Mucha J., Grunberger D., Chasin L. A.: BioTechniques *7*, 484 (1989).
34. Carothers A. M., Steigerwalt R. W., Urlaub G., Chasin L. A., Grunberger D.: J. Mol. Biol. *208*, 417 (1989).
35. Winter E., Yamamoto F., Almoguera C., Perucho M.: Proc. Natl. Acad. Sci. U.S.A. *82*, 7575 (1985).
36. Urlaub G., Mitchell P. J., Ciudad C. J., Chasin L. A.: Mol. Cell. Biol. *9*, 2868 (1989).
37. Strauss B. S.: Adv. Cancer Res. *45*, 45 (1985).